HIGH-TEMPERATURE SPECTROSCOPIC INVESTIGATION OF STIMULATED EMISSION FROM LASERS BASED ON CRYSTALS AND GLASSES ACTIVATED WITH Nd^{3+} IONS

A. A. KAMINSKIĬ

Institute of Crystallography, USSR Academy of Sciences

Submitted September 5, 1967

Zh. Eksp. Teor. Fiz. **54**, 727–750 (March, 1968)

A method of high-temperature spectroscopy of stimulated emission was used to study laser emission from 17 materials: CaF_2 type I and II, CaF_2–YF_3, CaF_2–CeF_3, CaF_2–SrF_2–BaF_2–YF_3–LaF_3, $2CaF_2$–$5YF_3$, SrF_2–LaF_3, BaF_2–LaF_3, α–$NaCaYF_6$, α–$NaCaCeF_6$, LaF_3, $CaWO_4$, $LaNa(MoO_4)_2$, and $Y_3Al_5O_{12}$, activated with Nd^{3+} ions, and also ruby and KGSS-7 and LGS-6 glasses. The high-temperature research made it possible to observe the effects of resonance high-temperature sensitization and flare-up of stimulated transitions, as well as the degeneracy of the generation line. The nature of the observed phenomena is discussed. The cross relaxation of energy among the optical centers in mixed fluoride crystals and glasses is confirmed experimentally. The investigation shows that the active media most suitable for high-temperature operation are mixed fluoride crystals; thus α–$NaCaYF_6$ lasers operate up to 1000°K.

INTRODUCTION

THE demands imposed on the active media of optically pumped solid state lasers have recently become more stringent. Quantum electronics today requires materials capable of broad practical utilization; they should have high efficiency, a broad operating temperature range, capability to radiate for a long time without detriment to the basic characteristics, etc. Separate studies of the optical spectra, output parameters of active media, and the technical application problems, as was done in the past, are no longer adequate. The complete set of data on a given material can now be obtained only in the course of a comprehensive research that includes the study of all the spectroscopic and generation characteristics within a broad temperature range, various methods of analyzing optical centers, the study of the mechanism of energy transfer and the kinetics of processes occurring in the excited state, etc. The entire research effort should be made in close association with the study of the physicochemical properties of the active materials and the problems of their technology.

At this time we know about 100 active laser materials[1-4]. One-third of this extensive list is capable of generation at room temperature; these materials are mainly crystals and glasses activated with Nd^{3+} ions. However numerous experimental situations call for media capable of laser action at higher temperatures. So far, almost all the spectroscopic studies of laser materials were performed within the temperature interval from 4.2 to 300°K; only a few cases dealing with specific problems[5,6] involved higher temperatures. Our preliminary high-temperature spectroscopic studies of stimulated emission from a series of crystals and glasses demonstrated their significance and capability to yield new information on the processes occurring in the course of laser generation. Our high-temperature experiments enabled us to observe new effects.

This work is a part of a research cycle on the study of new materials for lasers[1)] and is a continuation of[7]. It is intended to achieve two aims: first, to study the processes occurring at high temperatures in generating lasers based on simple and mixed fluoride systems as well as on compounds with complex oxygen-containing anions and on glasses activated with Nd^{3+} ions, and second, to determine the high-temperature limit of operation of these lasers.

INVESTIGATED CRYSTALS

For the investigation we used the crystals of CaF_2 (Type I), LaF_3, CaF_2–YF_3, BaF_2–LaF_3, SrF_2–LaF_3, CaF_2–CeF_3, CaF_2–SrF_2–BaF_2–YF_3–LaF_3, α–$NaCaYF_6$, and α–$NaCaCeF_6$ grown by the dropping crucible method in a metered fluoridizing atmosphere[8,9]. We also used the crystals of CaF_2 (Type II) containing oxygen ions in the optical centers. The crystals of $CaWO_4$, $LaNa(MoO_4)_2$ (c axis parallel to the geometric axis) and $2CaF_2$–$5YF_3$ were synthesized from the melt by the Czochralski method, and the crystals $Y_3Al_5O_{12}$ and Al_2O_3–Cr^{3+} were obtained by a method developed by the Institute of Crystallography of the USSR Academy of Sciences. The neodymium concentration in these media varied from 0.5 to 6% by weight. The grown single crystals were used to prepare specimens for the generation experiments in the form of circular cylindrical rods with plane parallel end faces. Some of the spectroscopic and generation characteristics of these crystals and the basic dimensions of the active elements are given in the table. We also used industrial glasses of the KGSS-7 and LGS-6 brands.

We note that the $2CaF_2$–$5YF_3$ crystals (of a rigorously stoichiometric composition) have a hexagonal structure in contrast with the CaF_2–YF_3 crystals[10].

[1)] This work was done together with Kh. S. Bagdasarov, Yu. K. Voronko, V. V. Osiko, and others.

Material	Nd^{3+} ion concentr. % by wt.	τ_{32} at 300°K sec	Rod length mm	Rod diamet. mm	Spectrum at 300°K, Å	High-temperature spectrum, Å	Average value of $\Delta\lambda/\Delta T$, 10^{-2} Å/deg: in parenth. T, °K	Temp. limit, °K
CaF_2 (typeI) [11]	0.5	0.7±0.06	75	6.5	*A* 10461	*A* 10461→10468 *G* 10628→10623	3.2 (520) ~2 (540)	530 560
CaF_2 (typeII) [12]	0.5	1.1±0.06	45	6.5	10885	10885→10889	3.3 (420)	480
CaF_2—YF_3 [13]	1	0.4±0.04	45	5.5	*A* 10461 B 10540 C 10632	— B 10540 C 10632→10603	— — 4.9 (900)	— 430 950
CaF_2—CeF_3 [14]	0.5	0.46±0.04	45	5.5	10657	10657→10640	4.2 (700)	750
CaF_2—SrF_2—BaF_2—YF_3—LaF_3 [15]	1	0.4±0.04	28	4.8	*A* 10535	*A* 10535→10547 C 10623→10585	4.8 (550) 9.5 (700)	550 700
$2CaF_2$—$5YF_3$	1	0.36±0.02	34	5	10498	10498	—	600
SrF_2—LaF_3 [16]	1	0.62±0.04	29	5	10597	10597→10583	2.8 (800)	900
BaF_2—LaF_3 [17]	0.5	0.5±0.04	45	6.1	10534	10534→10563	5.2 (850)	920
α-$NaCaYF_4$ [18]	1	0.36±0.02	29	6	B 10539 C 10629	B 10539→10549 C 10629→10597	4 (550) 4.9 (950)	550 ~1000
α-$NaCaCeF_4$ [19]	1	0.44±0.04	20	6	10653	10653→10633	4.3 (770)	920
LaF_3 [20]	1	0.66±0.04	32	6.2	*A* 10407 B 10633→10609 C 10591→10609	*A* 10407→10409 B 10633→10609 } D C 10591→10609	2.5 (380) ~4.6 (820) ~3.9 (820)	430 850 850
$CaWO_4$ [20]	1.5	0.18±0.01	45	4.5	10582	10582→10597	3.6 (720)	770
$LaNa(MoO_4)_2$ [21]	2	0.15±0.01	24	4.8	10653	10653→10665	3.1 (700)	750
$Y_3Al_5O_{12}$ [22]	1.5	0.22±0.01	62	5.2	10641	10641→10663	4.8 (760)	830
glass KGSS-7	6	0.4±0.04	38	4	~10595	10595→10628	~15 (520)	650
glass LGS-6	6	0.26±0.02	45	5	~10597	10597→10679	~33 (550)	600
Al_2O_3—Cr^{3+}	0.05	3.8±0.2	28	5.8	6943	6943→6952	~6 (450)	550

EXPERIMENTAL APPARATUS

We used a setup whose diagram is shown in Fig. 1. Reflector 1 of elliptical cross section served as the pump system. Its basic dimensions are 2a = 31 mm, 2b = 13.5 mm, 2c = 13.5 mm, and length is 90 mm. The interior surface was coated with silver. IPF-800 lamps were used as pump sources 2. Working crystal 3 was placed at the second focus of the reflector and was held by special tubular quartz holders 4. The crystal was heated by helical electric "furnace" 5 made of platinum wire 0.25 mm in diameter. Crystal temperature could be continuously regulared up to ~1100°K by varying the voltage of autotransformer 6. The temperature was controlled by chromel-alumel thermocouple 7 and an F-116/2 dc microvoltmeter. The thermocouple was calibrated by the usual method[23]. The accuracy of temperature measurements was 3–5% up to 600°K and 4–6% beyond.

The optical resonator consisted of external spherical mirrors 8 arranged confocally. The mirror transmission was ~0.7% at the generation wavelengths. To measure the output energy of generation a mirror was replaced by one having a transmission of 3% and over. The threshold generation energy was measured with an FÉU-28 photomultiplier and an S1-16 pulse oscilloscope. For lasers generating at several wavelengths the critical excitation energy of each line was determined by a similar photomultiplier placed at the output focal plane of a DFS-8 diffraction spectrograph (~5.9 Å/mm, resolution 600 lines/mm).

The spectral composition of stimulated emission was also studied with the aid of the DFS-8 instrument. The spectra were photographed on an I-1070 infrared film. The radiation of a lamp with an iron hollow cathode in the third order was used as reference.[2)]

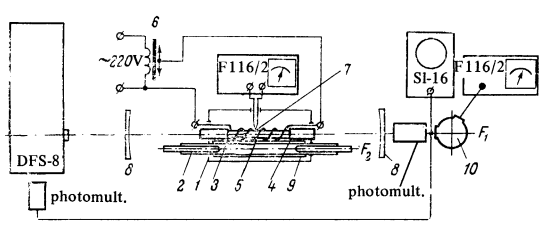

FIG. 1. Diagram of experimental setup

To avoid the undesirable "aging" effect[24,25] of Nd^{3+} ions in fluoride crystals in generation regime near 300°K the pump lamp was surrounded by a tubular filter 9 of ZhS-17 glass. The generation energy was measured with spherical calorimeter 10, 150 mm in diameter, with a thermopile. The interior surface of the calorimeter sphere was coated with white diffusing barium paint having a high reflection coefficient within the spectral range from 0.3 to 2μ. The F116/2 multirange high-resistance microvoltmeter was also used as the calorimeter indicator. The sensitivity of the calorimeter was $\sim 10^{-3}$ J.

The absorption and luminescence spectra and lifetimes of excited states were investigated with the DFS-12 diffraction spectrometer according to methods described in[22,26].

EXPERIMENTAL RESULTS

All the active media listed in the table can be divided into three groups in terms of the abundance of optical centers. The first group includes crystals that contain a small quantity of optical centers, not more than 5–7, with the usual laser activator concentration. These are crystals of CaF_2 Type I and II, LaF_3[3)], $CaWO_4$, $Y_3Al_5O_{12}$, and ruby. All mixed fluoride crystals and $LaNa(MoO_4)_2$ begin the second group of active media. In terms of their spectral characteristics they are close to glasses since they contain a large number of optical centers[27], and yet they are typical crystals in their structure. Activated glasses belong to the third group. The obtained experimental results are analyzed on the basis of the above classification.

A. Crystals with a Small Quantity of Optical Centers

$Y_3Al_5O_{12}$–Nd^{3+}. High-temperature spectra of stimulated emission from this crystal are shown in Fig. 2a for three temperatures. We see that a rise in tempera-

2)The author would like to thank A. I. Bodretsova who furnished the hollow cathode lamp for the experiments.

3)Only one type of optical center was observed by optical methods in tysonite crystals activated with Nd^{3+} ions.

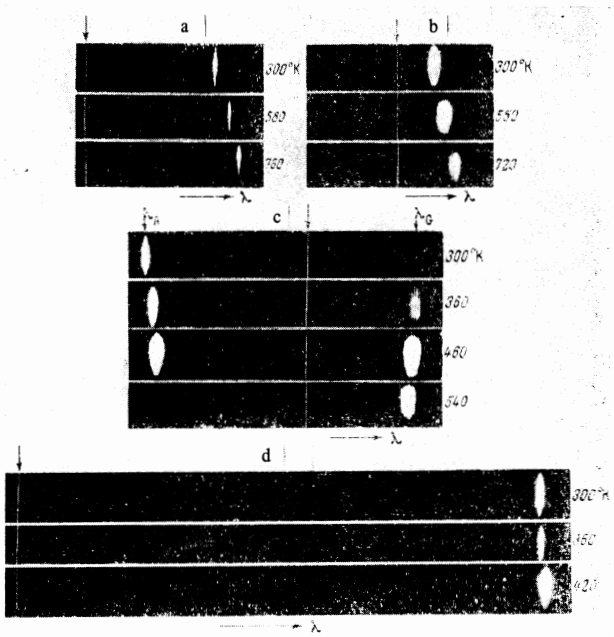

FIG. 2. High-temperature spectra of stimulated emission from Group I crystals activated with Nd^{3+}. a – $Y_3Al_5O_{12}$; b – $CaWO_4$; c – CaF_2 (Type I); d – CaF_2 (Type II). Arrows mark lines of the reference spectrum, λ = 10561.5 Å.

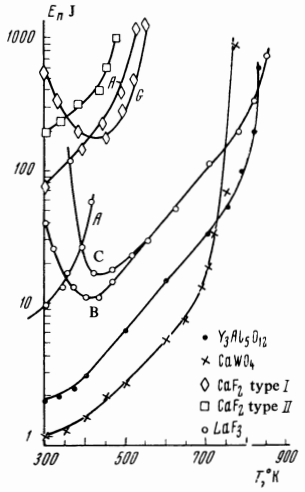

FIG. 3. High-temperature functions of the threshold energy of Group I crystals activated with Nd^{3+}.

ture shifts the generation wavelength in the direction of longer wavelengths at the rate $\Delta\lambda/\Delta T \approx 4.8 \times 10^{-2}$ Å/deg. The line width is practically unchanged in this process and remains equal to 0.9 ± 0.1 cm^{-1}. Figure 3 shows the threshold pump energy as a function of temperature $E_t(T)$. According to the figure, E_t begins to rise sharply at $T \sim 800$°K; at 830°K it was no longer possible to obtain laser action with our pumping system. The emission wavelength shifts from 10641 to 10663 Å within the interval from room temperature to ~760°K. It is of interest to note that the function $E_t(T)$ is linear from 400 to 800°K in our system of coordinates (see Fig. 3).

$CaWO_4$–Nd^{3+}. Figure 2b shows the spectra at high temperatures. The shape of the generation line is similar to the above case. With increasing temperature there is practically no line broadening ($\Delta\nu_D = 5.5 \pm 0.5$ cm^{-1}) but the line is shifted toward longer wavelengths at $\Delta\lambda/\Delta T \approx 3.6 \times 10^{-2}$ Å/deg. Figure 3 shows the function $E_t(T)$. In contrast to the garnet crystal, the limiting temperature of sheelite is ≈770°K. The linear portion of the $E_t(T)$ function is small, from 450 to 650°K.

CaF_2–Nd^{3+} (Type I). Investigation of the generation spectrum of this crystal at 300°K carried out earlier[11] revealed that it consists of a single line A with λ = 10461 Å associated with tetragonal optical centers[28]. Our high-temperature spectroscopic work revealed a still another line G (continuation of the alphabetic designation of generation lines of the CaF_2–Nd^{3+} Type I crystals[11]) with λ = 10628 Å that was not previously recorded because of the high excitation threshold. The high-temperature stimulated emission spectra of this crystal are shown in Fig. 2c and its $E_t(T)$ function in Fig. 3. Since the photograph of the generation spectrum was obtained from a single emission pulse the G line is absent from the spectrum corresponding to 300°K. At higher temperatures however the spectrum consists of two lines. It is apparent from Figs. 2 and 3 that lines A and G behave differently. The behavior of the A line is similar to that of the generation lines of garnet and scheelite. The G line has an entirely different behavior. In the first place as the temperature rises from 300°K to T ≈ 430°K E_t drops from 570 to 170 j. Further increase in temperature results in a sharp rise in E_t thus exhibiting an extremum. In the second place, the wavelength of the G line is shifted toward the short-wave side (10628 → 10623 Å) with increasing temperature. The limiting temperatures are 530°K for the A line and 560°K for the G line. As in the preceding cases the generation line widths change very little: $\Delta\nu_A = 3$–4.5 cm^{-1} and $\Delta\nu_G = 7.5$–10 cm^{-1}. The quantities $\Delta\lambda/\Delta T$ do differ slightly for these lines; this ratio equals $\approx 3.2 \times 10^{-2}$ for the A line and $\approx 2 \times 10^{-2}$ Å/deg for the G line.

CaF_2–Nd^{3+} (Type II). $E_t(T)$ and the generation line of this crystal (see Figs. 2d and 3) behave in the same way as those of garnet, scheelite, and the A line of the CaF_2–Nd^{3+} (Type I) crystal. Because of the high excitation threshold at 300°K the critical temperature is low for this crystal: ≈480°K. As the temperature rises the emission line shifts in the long wave direction (10885 → 10889 Å) at the rate of $\Delta\lambda/\Delta T \approx 3.3 \times 10^{-2}$ Å/deg. We observe in this crystal a marked thermal line broadening from ~1.5 to ~8 cm^{-1}.

LaF_3–Nd^{3+}. This crystal is the most interesting of all the active media of the first group under investigation. Its high-temperature spectra are shown in Fig. 4 and the $E_t(T)$ function in Fig. 3. When T = 300°K this crystal generates at two wavelengths A and B with λ = 10407 and λ = 10663 Å[29]. We see that the A line is present in the spectra only up to T ≈ 430°K and is practically unexcitable above this temperature. The B line behaves similarly to the G line of the CaF_2–Nd^{3+} (Type I) crystal, i.e., it has a minimum in the $E_t(T)$ function at 420–450°K. At T ≈ 350°K a third line C with λ = 10591 Å appears in the spectrum; this line cannot be excited at lower temperatures. Just as the B line, this line also has a thermal minimum of the excitation energy. The generation spectrum shows that with an increase in temperature the B and C lines first broaden considerably and then merge.

The unusual behavior of the generation line of the

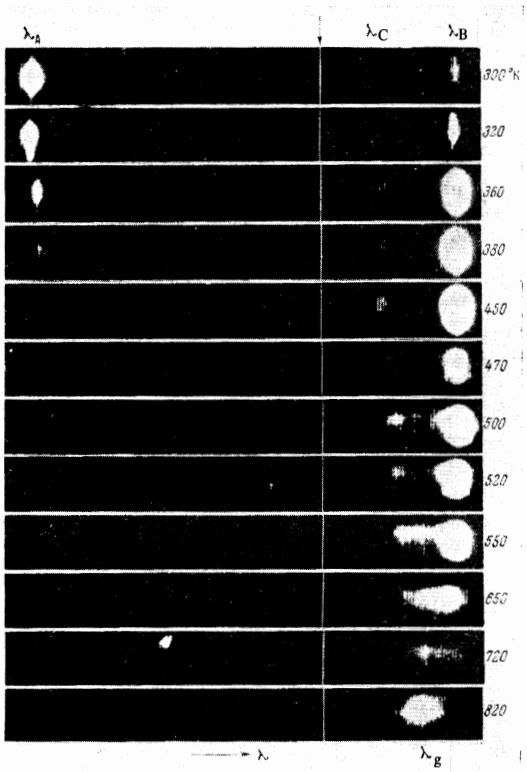

FIG. 4. Stimulated emission spectrum of the LaF_3-Nd^{3+} crystal. Arrow indicates reference line λ = 10561.5Å.

LaF_3–Nd^{3+} crystal can be explained by the crystalline splitting of the $^4F_{3/2}$ and $^4I_{11/2}$ terms that are directly involved in the generation transitions. The crystalline splitting diagram of these terms is given in Fig. 5. We see that stimulated transitions of A and B begin at the 11593 cm^{-1} lower level of the $^4F_{3/2}$ term and terminate at various Stark components of the $^4I_{11/2}$ term (1983 and 2189 cm^{-1}), while the C line connects the 11631 cm^{-1} upper level of the $^4F_{3/2}$ term with the same Stark component (2189 cm^{-1}) of the $^4I_{11/2}$ term that terminates the stimulated transition corresponding to the B line.

In contrast to the CaF_2–Nd^{3+} (Type I) crystal, a laser based on the LaF_3–Nd^{3+} crystals continues to generate at higher temperatures. As Figs. 4 and 3 show, at T ≈ 650°K there is a thermal merging of the lines and the spectrum contains only a single component D with λ = 10614 Å. A linear increase of $E_t(T)$ is observed up to T ≈ 780°K and the excitation threshold begins to rise sharply beyond this temperature. The limiting generation temperature of a laser based on lanthanum fluoride is ≈850°K. The ratio $\Delta\lambda/\Delta T$ equals 2.5×10^{-2} Å/deg for the A line and ~4.6 and 3.6×10^{-2} Å/deg for the B and C lines respectively.

B. Crystals of the Mixed Type with a Large Number of Optical Centers

CaF_2–YF_3–Nd^{3+}. According to the table, the yttrofluorite crystals can generate at three wavelengths: 10461, 10540, and 10632 Å[13]. The short-wave line is usually present in the spectra when the laser crystals contain a small quantity of YF_3 (0.1–1%) and Nd^{3+} (~0.5%). When the concentration of yttrium fluoride

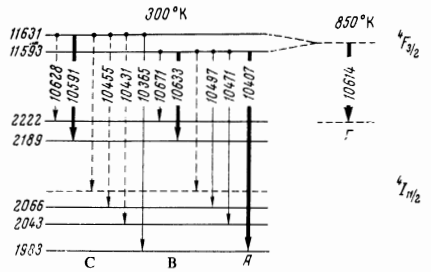

FIG. 5. Crystalline splitting of the $^4F_{3/2}$ and $^4I_{11/2}$ of the LaF_3–Nd^{3+} crystal. Position of levels is indicated in cm^{-1} and level transitions in Å. Heavy lines indicate stimulated transitions.

and neodymium is heavy only two long-wave lines remain in the spectrum. This is due to the fact that the concentration of tetragonal centers (see the CaF_2–Nd^{3+} Type I crystal[11]) emitting the A line at λ = 10461 Å is still high enough when the concentration of the above components is small. It was shown in[30] that the equilibrium of optical centers TR^{3+} shifts with increasing concentration of YF_3 and trivalent rare-earth elements (TR^{3+}). This is accompanied by a change in the concentration of the initial optical centers and by the appearance of new associates. In our experiments we used crystals that generated only two lines, B and C.

The high-temperature spectra of yttrofluorite are given in Fig. 6a and the functions $E_t(T)$ in Fig. 7. We see the usual behavior of the B line at λ = 10540 Å: a

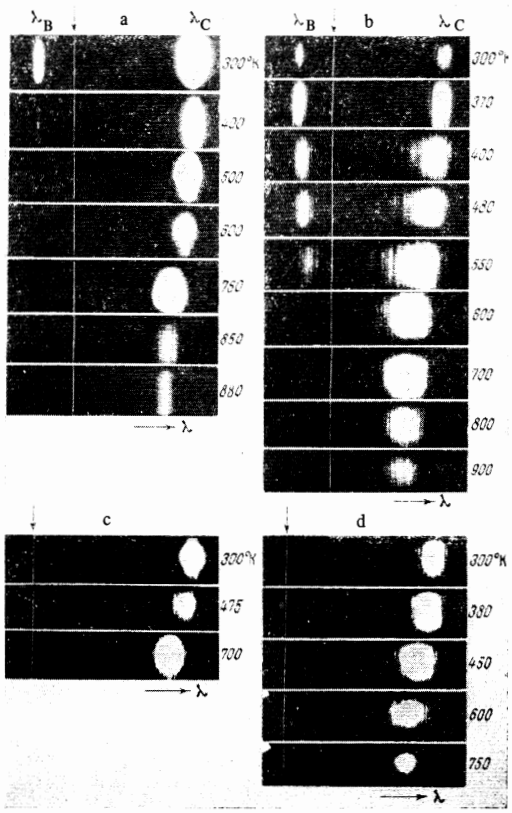

FIG. 6. High-temperature spectra of stimulated emission from Group II crystals activated with Nd^{3+}. a – CaF_2–YF_3; b – CaF_2–CeF_3; c – α-$NaCaYF_6$; d – α-$NaCaCeF_6$. Arrow indicates the reference spectrum line at λ = 10561.5 Å.

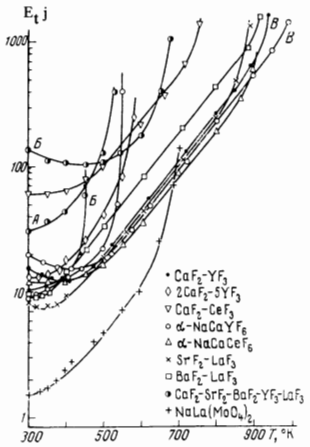

FIG. 7. High-temperature function $E_t(T)$ of Group II crystals activated with Nd^{3+}.

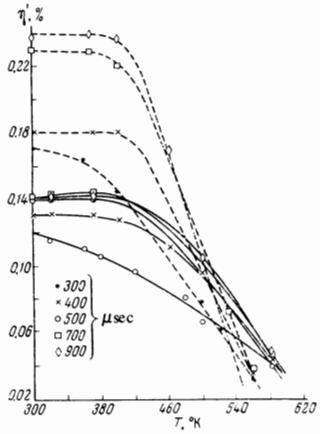

FIG. 8. Thermal dependence of efficiency of yttrofluorite lasers; Nd^{3+} ion concentration of 1% by weight (solid lines) and 2% by weight (dashed lines).

monotonic rise of the excitation threshold with increasing temperature. At $T \approx 430^\circ K$ a single C line at $\lambda = 10632$ Å remains in the spectrum. The $E_t(T)$ of this line has a minimum at $T \approx 430-450^\circ K$ although it is not so pronounced as in the case of CaF_2–Nd^{3+} (Type I). At 300°K the line is excited with a ~ 15.5 J input to the pump lamp. At the extremum of $E_t(T)$ the threshold energy is as low as 12.5 J. When the temperature is further increased to ~870°K $E_t(T)$ increases linearly in our coordinate system. The thermal operating limit of the yttrofluorite laser was ~950°K in our experiments. The generation spectrum shows that the C line wavelength shortens with increasing temperature to ~10600 Å at the rate of $\Delta\lambda/\Delta T \approx 4.9 \times 10^{-2}$ Å/deg. On the other hand, the B line behaves differently, shifting toward the longer wavelengths.

Figure 8 shows families of energy-dependent efficiency functions (ratio of generation energy to electrical energy supplied to the pump lamp) for lasers based on CaF_2–YF_3 crystals with various concentrations of the activator. The $\eta'(T)$ plots were obtained with an output mirror transmission of ~3% and various lengths of the pump light pulse ($\tau_{excit.}$) while the electrical input (~500 J) to the IFP-800 lamp was held constant. It can be seen that the nature of the $\eta'(T)$ functions changes with increasing τ_{excit} in crystals having a Nd^{3+} concentration of 1% by weight (solid lines). At $\tau_{excit.} = 300$ μsec, η' drops rapidly with increasing T. However, when τ_{excit} is long the output energy remains constant within a small temperature interval. We see that the efficiency is practically unchanged up to 400°K when $\tau_{excit.}$ increases from 400 to 900 μsec. In crystals whose concentration of Nd^{3+} ions is twice as high, the $\eta'(T)$ function is similar although the absolute value of efficiency is higher. The use of higher transmission (~10%) mirrors does not produce significant changes in the measurements of $\eta'(T)$.

$2CaF_2$–$5YF_3$–Nd^{3+}. While this crystal[4)] consists of the same ions as yttrofluorite it has a different, hexagonal type of crystalline structure. This difference substantially alters its spectroscopic characteristics. A laser based on this crystal emits at the wavelength of $\lambda = 10498$ Å at 300°K. Its $E_t(T)$ function is given in Fig. 7. Unfortunately we had only a single crystal for the experiments and it was destroyed in the course of the work. This prevented us from investigating all its high-temperature characteristics. The critical generation temperature was estimated at ~600°K.

CaF_2–CeF_3–Nd^{3+}. The high-temperature stimulated emission spectra from fluocerite are given in Fig. 6b. As the temperature increases the generation wavelength shrinks from 10657 to 10640 Å ($\Delta\lambda/\Delta T \approx 4.2 \times 10^{-2}$ Å/deg) while the line width changes very little. Thus the value of $\Delta\nu_g \approx 7$ cm^{-1} at $T \approx 300^\circ K$ and increases only to ~13 cm^{-1} at T = 700°K. Figure 7 shows the $E_t(T)$ function. Since the optical quality of the investigated fluocerite crystals was unsatisfactory the initial value of E_t was found to be high enough. It is apparent that the excitation threshold is practically unchanged up to $T \approx 400^\circ K$. At higher temperatures the nature of $E_t(T)$ is very close to the cases discussed above. The temperature limit for fluocerite in our experiments was ~750°K.

We note one significant consideration. While the CaF_2 and CaF_2–YF_3 crystals with Nd^{3+} ions "age" rapidly when exposed to the high-power pulses of the pump lamp[6,24,25], the fluocerite crystals show no such effect. This is due to the fact that the Ce^{3+} ions embedded in the crystal are strongly absorbing in the short-wave region and thus protect the working Nd^{3+} ions from the ultraviolet radiation of the pump lamp.

α-NaCaYF$_6$–Nd^{3+} (α-gagarinite). Of all the investigated crystals and glasses α-gagarinite with Nd^{3+} ions is the most high-temperature resistant active material. According to Fig. 7, a laser based on this crystal can emit at $T \approx 1000^\circ K$. The high-temperature investigation of $\eta'(T)$ showed that the generation properties of the laser are not impaired up to $T \approx 450^\circ K$. The spectral composition of stimulated emission from this crystal is very close to that of yttrofluorite. At 300°K it consists of two lines B and C with wavelengths of 10539 and 10629 Å respectively (Fig. 6c). The B line is present in the generation spectrum up to $T \approx 550^\circ K$. The $E_t(T)$ function of the C line has a minimum at $T \approx 430-460^\circ K$ just as in the case of the C line of yttrofluorite. This extreme is somewhat broader than in the case of the CaF_2–YF_3–Nd^{3+} crystal. The functions $E_t(T)$ and $\eta'(T)$ are in an adequate agreement with each other.

Figure 9 shows the generation line widths of

[4)] Lasing action in $2CaF_2$-$5YF_3$–Nd^{3+} crystals was first obtained by Yu. K. Voronko, R. G. Mikaelyan, V. V. Osiko, and V. T. Udovenchik.

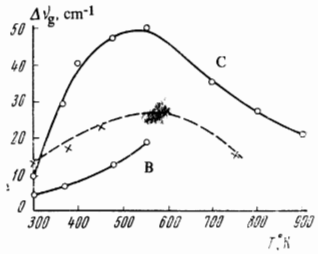

FIG. 9. Thermal dependence of the width of the B and C generation lines in the α-$NaCaYF_6$ (solid lines) and α-$NaCaCeF_6$ (dashed line) crystals.

α-gagarinite with Nd^{3+} ions. The following interesting fact should be considered here. The B line is shifted toward the longer wavelengths up to $\lambda = 10549$ Å at the rate of $\Delta\lambda/\Delta T \approx 4 \times 10^{-2}$ Å/deg; the line broadening is not symmetric however but is mainly due to the short-wave wing. The C line on the other hand shifts toward the short wave side up to $\lambda = 10597$ Å at $\Delta\lambda/\Delta T \approx 4.9 \times 10^{-2}$ Å/deg and is broadened by the short wave wing. The function $\Delta\nu_g(T)$ has an extremum at $T \approx 550^\circ$K.

α-$NaCaCeF_6$-Nd^{3+}. The structure of this crystal is close to that of α-gagarinite. Its emission spectra are given in Fig. 6d and the $E_t(T)$ function in Fig. 7. The thermal limit of generation is seen to equal ~920°K. When the temperature increases the emission line shortens from $\lambda = 10653$ Å (300°K) to $\lambda = 10633$ Å at the rate $\Delta\lambda/\Delta T \approx 4.3 \times 10^{-2}$ Å/deg. At moderate temperatures the $E_t(T)$ function is of the same character as the fluocerite function, i.e., the excitation threshold is practically unchanged up to $T \approx 400^\circ$K. The $\Delta\nu_g(T)$ function has an extremum at $T \approx 500$–550°K (see Fig. 8). As in the case of CaF_2–CeF_3–Nd^{3+} these crystals are subject to marked "aging" when exposed to the pump lamp light pulses.

SrF_2–LaF_3–Nd^{3+}. The temperature-dependent function of E_t for a laser based on strontium-lanthanum fluoride activated with Nd^{3+} ions is shown in Fig. 7. It can be seen that $E_t(T)$ also has a minimum but at $T \approx 350$–360°K. At higher temperature $E_t(T)$ has the same shape as in other fluoride crystals. Our experiments showed that the thermal limit of SrF_2–LaF_3–Nd^{3+} is ~900°K. The extremum of the $E_t(T)$ function is less pronounced in these crystals than in the above cases. The high-temperature generation spectra of the SrF_2–LaF_3–Nd^{3+} crystal are shown in Fig. 10a. Near room temperatures the spectrum consists of a broad line at 10597 Å with $\Delta\nu_g \approx 24$ cm^{-1} and a weak line at $\lambda = 10568$ Å ($\Delta\nu_g \approx 7$ cm^{-1}) adjacent on the short-wave side to the former. As the temperature increases this line rapidly merges with the main line. Unlike other crystals, the spectrum of SrF_2–LaF_3–Nd^{3+} remains practically unchanged with increasing temperature. While there is a shift of the generation line toward shorter wavelengths, it is very negligible. Thus at $T = 800^\circ$K $\lambda = 10583$ Å, i.e., $\Delta\lambda/\Delta T = 2.8 \times 10^{-2}$ Å/deg. The emission line width also changes little and remains equal to $\Delta\nu_g \approx 22$ cm^{-1}.

BaF_2–LaF_3–Nd^{3+}. The $E_t(T)$ function of this crystal is analogous to that of SrF_2–LaF_3–Nd^{3+} (see Fig. 7) although the extremum occurs at a temperature as low as ~320–330°K. The temperature limit of generation is ~920°K. The generation spectra are shown in Fig. 10b. At 300°K a barium-lanthanum fluoride Nd^{3+} laser emits at the wavelength of 10534 Å.

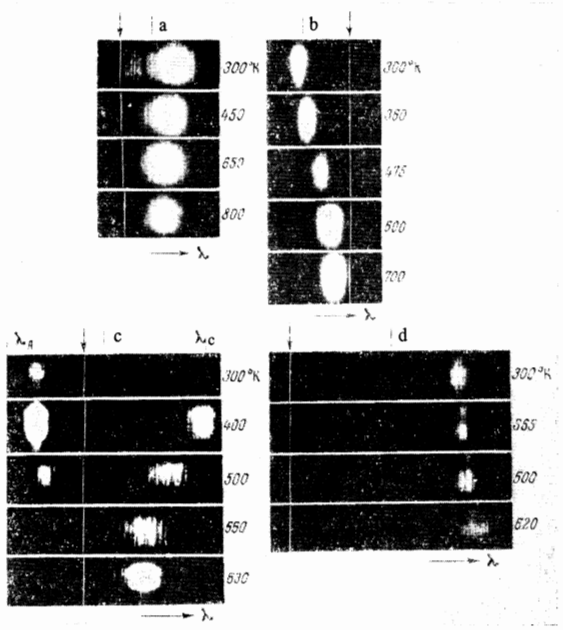

FIG. 10. Stimulated emission spectra of Group II crystals. a – SrF_2–LaF_3; b – BaF_2–LaF_3; c – CaF_2–SrF_2–BaF_2 YF_3–LaF_3; d – $LaNa(MoO_4)_2$. Arrow indicates reference line at $\lambda = 10561.5$ Å.

An increase of temperature shifts the stimulated emission line in the direction of longer wavelengths up to $\lambda = 10563$ Å (~850°K) at the rate of $\Delta\lambda/\Delta T \approx 5.2 \times 10^{-2}$ Å/deg. At 700°K the generation line width is approximately twice as broad as at 300°K and equals ~17 cm^{-1}.

Figure 11 shows the experimental plot of the $\eta'(T)$ function for the BaF_2–LaF_3–Nd^{3+} crystal. As we see the output energy rapidly drops with increasing T and the optimum length of the pumping pulse is 400—500 μsec.

CaF_2–SrF_2–BaF_2–YF_3–LaF_3–Nd^{3+}. The high-temperature stimulated emission spectra of this crystal are given in Fig. 10c and the $E_t(T)$ function in Fig. 7. At 300°K a single line A only at $\lambda = 10535$ Å was previously observed[15,31] in the emission spectrum of the five-component fluoride. The width of this generation line is practically unchanged within the temperature interval from 300 to 550°K and equals ~7 cm^{-1}.

Our investigations revealed a new line C at $\lambda = 10623$ Å. Its $E_t(T)$ function at 300°K is almost five times higher than the E_t function of the A line. It is apparent from Fig. 10 that the $E_t(T)$ function of this line has a very broad extreme at $T \approx 450$–480°K. The ratio of E_t at 300°K to E_t at the extremum is ~1.35. With increasing temperature the C line shifts toward short waves at the rate $\Delta\lambda/\Delta T \approx 9.5 \times 10^{-2}$ Å up to $\lambda = 10585$ Å. The temperature limit for the C line is ~700°K. Its width is also practically unchanged within a broad interval of temperatures and amounts to 25 ± 2 cm^{-1}.

$LaNa(MoO_4)_2$–Nd^{3+}. This crystal also belongs to the mixed crystal category characterized by an abundance of optical centers[21]. Its high-temperature spectra are shown in Fig. 10d and the $E_t(T)$ function in Fig. 7. The generation parameters of a laser based on this crystal are close to those of a scheelite laser.

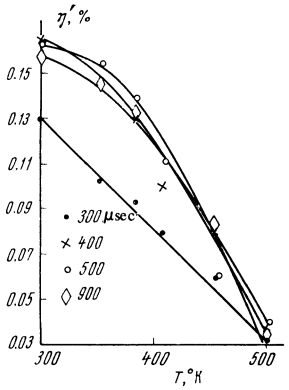

FIG. 11. Thermal dependences of efficiency of BaF_2–LaF_3–Nd^{3+} (0.5% by weight of Nd^{3+}) lasers.

In spite of the low threshold at 300°K, equal to ~1.6 J, its temperature limit is ~750°K. With increasing temperature the λ = 10653 Å emission line shifts toward long wavelengths at the rate of $\Delta\lambda/\Delta T \approx 3.1 \times 10^{-2}$ Å/deg up to 10665 Å (700°K) while $\Delta\nu_g$ increases from 5.5 to 16 cm^{-1}.

C. Activated Glasses.

The KGSS-7 glass. High-temperature stimulated emission spectra from this active material are shown in Fig. 12a and the $E_t(T)$ function in Fig. 13. We see that E_t rapidly rises with increasing T and at 650°K generation is impossible to stimulate with out pumping system. At 300°K the emission spectrum consists of a broad line with $\Delta\nu_g \approx 60$ cm^{-1} at λ_{center} = 10595 Å. Increasing temperature shifts the line toward long wavelengths at $\Delta\lambda/\Delta T \approx 15 \times 10^{-2}$ Å/deg; the width of the line shrinks rapidly in the process, so that at T ≈ 520°K λ_{center} = 10627 Å and $\Delta\nu_g \approx 20$ cm^{-1}. The line narrowing occurs at the short-wave wing. The $\Delta\nu_g(T)$ function is shown in Fig. 14a.

The LGS-6 glass. The $E_t(T)$ function of this brand of glass is close to that of the above case (see Fig. 13). The high-temperature spectra are given in Fig. 12b. The stimulated emission wavelength varies from λ_{center} = 10597 Å (300°K) to λ_{center} = 10769 Å (550°K) at $\Delta\lambda/\Delta T \approx 33 \times 10^{-2}$ Å/deg. The relative thermal shift of the generation line of this glass is almost twice as high as in the case of the KGSS-7. The

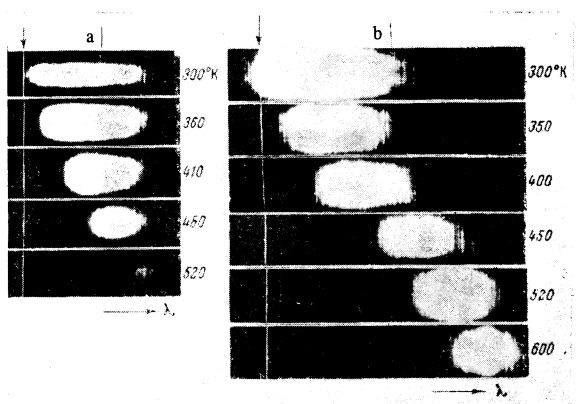

FIG. 12. High-temperature stimulated emission spectra of neodymium glasses. a – KGSS-7; b – LGS-6. Arrow indicates the reference spectrum line at λ = 10561.5 Å.

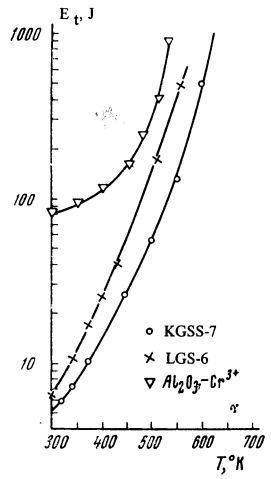

FIG. 13. High-temperature dependences of the threshold energy of neodymium glasses and ruby.

thermal dependence of the emission line width is shown in Fig. 14b.

Figure 15 shows the $\eta'(T)$ function of a laser based on the LGS-6 glass at various pumping pulse lengths. The functions shown were obtained when the transmission of the output mirror was 3% and the electrical energy supplied to the IPF-800 lamp was held constant (~500 J).

DISCUSSION OF RESULTS

Our research shows that as the temperature of the active material increases the threshold excitation energy of most media monotonically increases until a definite critical value is reached. The $E_t(T)$ plot of many crystals has a linear region (in our coordinate system). According to our analysis the $E_t(T)$ plots have a common characteristic within this region: the lines are parallel. This gives us reason to assume that generation processes occurring in the corresponding temperature intervals have a common nature.

Before turning to the discussion of other experimental data we make a rough analysis of the thermal dependence of E_t for the case of a four-level laser in which the terminal level population is variable: $N_2(T)$. The levels are numbered in the order of increasing energy. If the stimulated transition connects levels 3 and 2 the generation threshold corresponds to the following equality:

$$\Delta N = N_3\frac{g_2}{g_3} - N_2 = \frac{Kv}{B_{23}h\nu_{32}g(\nu_{32})}, \qquad (1)$$

where N_2 and N_3 are the numbers of particles at the corresponding levels per unit volume, g_2 and g_3 are statistical weights of the levels (we assume that g_2

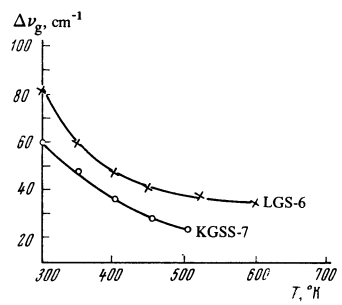

FIG. 14. Thermal dependences of generation bandwidths for neodymium glasses.

$= g_3 = 1$), ν_{32} is the stimulated transition frequency, $K = l^{-1} \ln R^{-1}$ are optical resonator losses (in this formula l is the length of the resonator: we further assume that the reflection coefficient R of the mirrors is the same and that losses due to crystal inhomogeneities are absent), v is the velocity of light in the active medium, $g(\nu_{32})$ is the form factor of the line also assumed equal to $1/\Delta\nu_{32}$ (here $\Delta\nu_{32}$ is the line width of the working transition luminescence), B_{23} is the Einstein coefficient, and h is the Planck constant. Since [32]

$$B_{23} = A_{32}\frac{g_3 c^3}{8\pi g_2 h \nu_{32}^2 n'^3},$$

the threshold difference of working level populations can be written as

$$\Delta N = \frac{8\pi\Delta\nu_{32}\ln R^{-1}}{A_{32} l \lambda_{32}^2}, \qquad (2)$$

where n' is the refraction coefficient of the active medium.

The threshold density U^t of the pumping radiation can be determined from the solution of kinetic equations (see for example [33]) assuming that

$$p_{13}^0 = p_{14}^0 = p_{23}^0 = p_{24}^0 = p_{34}^0 = 0, \quad p_{12}^0 = p_{21}^0 \exp(-h\nu_{21}/kT),$$
$$U_{21} = U_{31} = U_{32} = U_{42} = U_{43} = 0 \quad (U_{41} \neq 0),$$
$$B_{14}U_{41} \ll A_{41}, \quad B_{14} = B_{41},$$
$$p_{43}^0 \gg p_{42}^0, \quad p_{21}^0 \gg p_{32}^0 + p_{31}^0, \quad p_{43}^0 \gg p_{31}^0 + p_{32}^0. \qquad (3)$$

Here p^0_{mn} is the transition probability for the case of thermodynamic equilibrium and U_{mn} is the external radiation density at the frequency ν_{mn}. We have

$$U_{14}^t B_{14} = \frac{1}{\eta}\frac{(p_{31}^0 + p_{32}^0)[(N+\Delta N)\exp(-h\nu_{21}/kT) + \Delta N]}{N - \Delta N}, \qquad (4)$$

where $\eta = p^0_{43}/(p^0_{41} + p^0_{42} + p^0_{43})$.

Since the "height" of level 2 depends on T in our case we consider that $N_2 = N_1 \exp(-h\nu_{21}/kT) \neq 0$, $N_3 = N_2 + \Delta N$, and $N = N_1 + N_2 + N_3$; then $N - \Delta N = N_1[1 + 2\exp(-h\nu_{21})kT]$. We perform the appropriate operations in (4) and considering that $\Delta N \ll N$ and also assuming that $p^0_{31} \ll p^0_{32} = A_{32}$ we obtain

$$U_{14}^t B_{14} = \frac{A_{32}}{\eta}\frac{\Delta N + N\exp(-h\nu_{21}/kT)}{N_1[1 + 2\exp(-h\nu_{21}/kT)]}. \qquad (5)$$

In view of the approximate nature of our analysis we consider that the entire incident radiation $U_{14}B_{14}$ is absorbed in the crystal. The threshold value of pumping power per unit volume of the active material is then expressed by

$$P_{14}^t = h\nu_{14} N_1 U_{14}^t B_{14} = \frac{h\nu_{14}}{[1 + 2\exp(-h\nu_{21}/kT)]\eta}$$
$$\times\left[\frac{8\pi^2\Delta\nu_{32}\ln R^{-1}}{l\lambda_{32}^2} + A_{32} N \exp\left(-\frac{h\nu_{21}}{kT}\right)\right]. \qquad (6)$$

This equation can be simplified somewhat. When R is close to unity $\ln R^{-1} = 0.5(1 - R^2)$, also $[1 + 2\exp(-h\nu_{21}/kT)] \approx 1$ up to 1000°K for the Nd^{3+} ion; furthermore considering that A_{32} is inversely proportional to the radiative lifetime of level 3 ($A_{32} = \tau_{32}^{-1}$) we write (6) in the form

$$P_{14}^t = \frac{h\nu_{14}}{\eta}\left[\frac{4\pi^2(1-R^2)\Delta\nu_{32}}{l\lambda_{32}^2} + N\tau_{32}^{-1}\exp\left(-\frac{h\nu_{21}}{kT}\right)\right]. \qquad (7)$$

This equation is valid for the stationary state, i.e., for the case where the length of the exciting pulse is greater than the period of stabilization of the generation process. We see that P_{14} depends on η, $\Delta\nu_{32}$, τ_{32}, and temperature. At low temperatures the last term in parentheses tends to zero and (7) converts to a well-known simple relationship P^t_{14} for a four-level laser with a "high" terminal level [34]. Unfortunately an analysis of the function $P^t_{14}(\eta, \Delta\nu_{32}, \tau_{32})$ is difficult at present due to the lack of experimental data on the thermal dependencies of η, $\Delta\nu_{32}$ and τ_{32} [5].

Of greatest interest are cases where the length of the exciting pulse is considerably shorter than or comparable to the generation stabilization period. As shown in [35] the following relationship should be valid for the first case: $E^t_{14} = P^t_{14}\tau_{32}$ or in our case

$$E_{14}^t = \frac{h\nu_{14}}{\eta}\left[\frac{4\pi^2\tau_{22}\Delta\nu_{32}(1-R^2)}{l\lambda_{32}^2} + N\exp\left(-\frac{h\nu_{21}}{kT}\right)\right]. \qquad (8)$$

The table shows that τ_{32} at 300°K is equal to ~400 μsec on the average. Our experiments in measuring $E_t(T)$ were performed with an exciting pulse length of 50–200 μsec, thus realizing the case corresponding to (8). However τ_{32} can shorten with increasing temperature while the length of τ_{excit} remains unchanged or is increased since $E_t(E = CU^2/2)$ increases. As a result at some high temperature the pulsed generation mode ($\tau_{excit} < \tau_{stab}$) can change into a quasistationary or a continuous ($\tau_{excit} \geq \tau_{stab}$) mode. Therefore the above expressions for threshold energy are valid only in very rough analysis and only for specific temperatures. More accurate computation of E_t requires the solution of a system of velocity equations taking variable temperature into account.

Numerical solutions of (7) and (8) carried out on the assumption that η, $\Delta\nu_{32}$, and τ_{32}, vary negligibly with increasing T showed that the first term in brackets makes the principal contribution to the threshold excitation energy at a concentration of active particles of $N \approx 10^{19}$ cm^{-3}. In our crystals (see the table) the concentration of active particles amounts to ~10^{20} cm^{-3} and the exponential term can no longer be neglected even at temperatures close to 300°K.

Turning back to Figs. 3, 7, and 13 we see that almost all the fluoride crystals are capable of stimulated emission at higher temperatures than is the case with oxygen-containing crystals and glasses although the latter have a lower threshold at 300°K.

In the case of the crystals of CaF_2 (Type I), LaF_3, CaF_2–YF_3, SrF_2–LaF_3, BaF_2–LaF_3, α-$NaCaYF_6$, and the five-component fluoride, we already noted above a decrease of the excitation threshold at high temperatures. Analyzing this phenomenon we have concluded that the minima of $E_t(T)$ correspond adequately to the

[5] The recent preliminary results of high-temperature investigation of the lifetimes τ_{32} of crystals and glasses activated with Nd^{3+} ions, whose stimulated emission is discussed in this paper, indicate that the metastability of the initial generation levels varies negligibly within a wide temperature interval from 300 to 800°K. Thus for example τ_{32} of the LaF_3–Nd^{3+} (1%) crystals is ~670 μsec at 300°K; this time shortens only to ~600 μsec when the temperature is increased to 800°K. In the case of LGS-6 glasses at 300°K τ_{32} = 230 μsec dropping to ~180 μsec at 800°K. For $CaWO_4$–Nd^{3+} (2%) and $Y_3Al_5O_{12}$–Nd^{3+} (1%) the time τ_{32} at 300°K is ~180 and ~220 μsec and at 800°K it is as low as ~140 and ~150 μsec. The lifetime of Al_2O_3–Cr^{3+} (0.05%), unlike the Nd^{3+} -containing media, decreases more at higher temperatures: thus the τ_{32} time equal to ~3.8 μsec at 300°K shortened to ~1.2 μsec at 700°K.

characteristic Debye temperatures (T_D) of the crystals. Unfortunately an experimental measurement of T_D was performed only for the simple compounds: CaF_2, SrF_2, BaF_2, and LaF_3. Furthermore the lack of more complete data on T_D is not the only problem besetting our analysis of the other crystals.

As we know the characteristic temperatures of crystals are mainly computed from known elastic constants and from the heat capacity[36,37] or they are estimated from the melting points[38]. Because of this there is a considerable spread of the values of T_D reported by various authors. Thus T_D for CaF_2 was determined from elastic constants as 474°K in[39] and as 515°K in[40]. In[40] the value of T_D was also computed from heat capacity and found to be ≈508°K. The temperature $T_D \approx 380$°K for the SrF_2 crystal[41] and $T_D = 282$°K for barium fluoride[42]. These characteristic temperatures were also computed from elastic constants. For tysonite the Debye temperature was estimated from the study of vibrational spectra in[43]. The authors of that work report the value of $T_D \approx 360$°K and at the same time indicate that the actual value of the Debye temperature can be somewhat higher.

A decrease of E_t with increasing T reported in[7] was due to resonance oscillations of crystals at $T = T_D$. According to Kiel's theoretical analysis[44] thermal oscillations of the crystal can significantly change the probabilities of electron transitions of TR^{3+}. If this is true then their effect should rise sharply when $T = T_D$. The experimental results given above allow us to assume that the threshold depression is connected with the Debye temperature. A particularly strong verification of this assumption is afforded by the high-temperature spectroscopic data for the LaF_3–Nd^{3+} crystal. Figure 3 shows that the B generation line is excited at E = 143 J at 300°K. E_t begins to decrease when the temperature increases. It follows from (7) and (8) that E_t depends on ΔN, τ_{32}, η, and $\Delta\nu_{32}$. As T increases the last three parameters merely cause an increase of E_t. This is in good agreement with the behavior of the A generation line (see Fig. 3): it has a common initial level (11593 cm^{-1} of the $^4F_{3/2}$ term, see Fig. 5) with the B line. On the other hand the useful population difference ΔN between levels 3 and 2 participating in generation strongly depends on the probability of transitions from the terminal level at 2189 cm^{-1} to the ground level, i.e., on the rate of relaxation τ_{34}. Since the depletion of levels of the $^4I_{11/2}$ term is only due to the nonradiative transitions[45] it is entirely correct to assume that at $T = T_D$ resonance oscillations of the crystal cause a drastic shortening of time τ_{34}; this can also be enhanced by virtue of multiphonon relaxation processes.

The nature of this phenomenon is similar to the disappearance of the "bottleneck" in paramagnetic relaxation processes. This assumption is verified by experimental fact that resonance oscillations in tysonite crystals lead to an improvement of conditions for stimulated emission. This is why the phenomenon observed in[7] was called the thermal resonance sensitization process.

This effect is also observed in the CaF_2–Nd^{3+} (Type I) crystals in the new G line observed by us. Unfortunately it is difficult to identify it with respect to the L, M, and N centers[28] since this line is very weak in the luminescence centers. Therefore it is now not possible to carry out an analysis similar to that performed for the LaF_3–Nd^{3+} crystal. The minimum of $E_t(T)$ for this line does not quite correspond to T_D[39,40]. On the other hand, this discrepancy can be due to the different technology characterizing our crystals that is capable[1,2] of strongly affecting their physical properties. At moderate values of T however the extreme of $E_t(T)$ can be determined by thermal sensitization and at $T \approx 450$°K the value of E_t can already be strongly dependent on the quite probable changes of η, τ_{32}, or $\Delta\nu_{32}$, for example. And this in the final analysis can "shift" the minimum toward low temperatures.

There are no data on the variation of T_D for mixed crystals (CaF_2–YF_3, SrF_2–LaF_3, BaF_2–LaF_3, α–$NaCaYF_6$, and CaF_2–SrF_2–BaF_2–YF_3–LaF_3); however assuming that these systems mainly consist of fluorides of Ca, Sr, and Ba and considering their melting points we can assume that their characteristic temperatures will not strongly differ from the T_D values of simple crystals. The series CaF_2–YF_3, SrF_2–LaF_3, BaF_2–LaF_3 is interesting in this respect. According to Fig. 7 their $E_t(T)$ functions also have minima although this time subject to a definite regularity: first, there is a shift of the minima toward low temperatures and, second, the extremum itself is less pronounced, i.e., there is a reduction in the ratio of E_t at room temperature to E_t at the extremum point. The high-temperature behavior of the $E_t(T)$ function in α-gagarinite and the five-component fluoride is similar to that in CaF_2–YF_3.

The second unique property of the LaF_3–Nd^{3+} crystal is the appearance of a new generation line C at $T \approx 360$°K. It is apparent from the $E_t(T)$ plot for the C line (see Fig. 3) that it cannot generate at room temperature. The flare-up of the new stimulated emission is obviously due to the thermal population of the upper component of the $^4F_{3/2}$ term (see Fig. 5). However, considering the fact that the probability of transitions from the terminal level (2189 cm^{-1}) can sharply rise at T_D we can be sure that this phenomenon depends on the complex of processes that occur at high temperatures. It is also quite obvious that the probabilities of transitions from the components of the $^4F_{3/2}$ term to the 2189 cm^{-1} level of the $^4I_{11/2}$ term are similar, or else we would see "jumps" in the generation frequency with temperature changes as in the case of the $Y_3Al_5O_{12}$–Nd^{3+}[33] crystals. The equality of transition probabilities at the $^4F_{3/2}$ components leads to the interesting case of degeneracy of stimulated transitions.

The oxygen-containing crystals of $Y_3Al_5O_{12}$, $CaWO_4$, and $LaNa(MoO_4)_2$ show a characteristic rapid rise of E_t at the temperatures of ~800, 720, and 680°K respectively, according to Figs. 3 and 7. Juxtaposing the $E_t(T)$ function with T_D of these crystals (the value of $T_D = 700$–750°K for $Y_3Al_5O_{12}$[46] and T_D 680°K for $CaWO_4$[6)] we see that the sharp increase of E_t occurs

[6)] The values of T_D for $CaWO_4$ were determined by G. P. Shipulo and V. A. Sychugov by analysing the thermal shift of the generation line at low temperatures.

precisely at $T = T_D$. It is difficult to say at this time whether the T_D factor of these crystals has a direct effect on the energy relaxation processes although such a possibility cannot be ruled out. For example the increase in the probabilities of nonradiative transitions from the initial level of the $^4F_{3/2}$ term or from higher levels can cause a reduction of η and ΔN. All this guesswork of course requires a thorough experimental verification. As for the fluocerite crystals and α-$NaCaCeF_6$, the behavior of their $E_t(T)$ functions near 300°K remains invariant.

A comparison of the $\eta'(T)$ functions for the investigated active media (see Figs. 7, 11, and 15) shows that the mixed fluoride crystals possess the remarkable property of retaining their output energy characteristics up to the temperatures somewhat over 400°K. This property is of considerable value for possible applications. Figures 8 and 11 also show that the quantity η' is strongly affected by the length of the pumping pulse τ_{excit}. This indicates the fact that the migrations of energy among various optical centers play a significant role in the mixed systems. A similar effect is observed in glasses (see Fig. 15). These results are in good agreement with the data presented in [47] concerning the study of stimulated emission in Q-switched modes.

In addition to the valuable property to retain η' invariant within a broad range of temperatures, the mixed fluoride crystals are characterized by high efficiency. A comparison of the η' values of the investigated glasses with the data for mixed fluoride crystals shows a negligible difference in efficiency. At the same time we note that the activator concentration is lower in mixed crystals than in glasses.

As we known [3,4], glass lasers have broad emission spectra reaching ~50 cm^{-1} in width at near threshold pumping energy. This broad emission band of neodymium glasses is caused by Nd^{3+} ions situated in irregular ligand fields (abundance of optical centers [4]). Another characteristic property of glasses is that at the pumping energy close to E_t the generation spectra consist of a large number of narrow lines whose position in the emission band changes from pulse to pulse. This is apparently due to the fact that there are groups of centers with similar conditions of stimulated emission but ineffective coupling between the generating centers. The narrowing of the KGSS-7 and LGS-6 laser generation spectrum observed by us at high temperatures (this also seems to be typical of other glasses) indicates an increasing probability of energy migration among the emitting centers.

An analogous situation is observed in mixed fluoride crystals. Although inhomogeneous broadening of the optical spectral lines has the same characteristics as in glasses the resonance interaction among the optical centers is stronger in this case. This is indicated by the quantities η' and $\Delta\nu_g$, and the function $\Delta\nu_g(T)$. It does not follow from our results that the autoresonance interaction is strengthened with increasing T. However we performed additional experiments, whose results will be published elsewhere, to study the migration of energy among the optical centers at high temperatures; the experimental results show that the effectiveness of energy transfer increases at $T = T_D$ in some systems.

The high-temperature stimulated emission spectra show that the laser frequency can be varied significantly by changes in temperature. In many lasers this causes a negligible change in $\Delta\nu_g$.

As was noted above mixed crystals are characterized by an abundance of optical centers. This property is reflected in the broad bands of their optical spectra that cannot be resolved under any conditions. This is also true of glasses. The search for crystals with good generating properties requires information on the most "active" optical centers. We think that the method of high-temperature stimulated emission spectroscopy described in this paper can prove useful in this respect. The analysis of high-temperature stimulated emission spectra of structurally close crystals of CaF_2–YF_3, α-gagarinite, and the five-component showed that the behavior of the C generation line is common to all. The same situation is observed in the series CaF_2–CeF_3 and α-$NaCaCeF_6$. This indicates the regardless of the different chemical composition of these crystals, they have structurally similar groups of optical centers. If this is true then we have the means to recommend for synthesis mixed systems with suitable generation properties.

The high-temperature experiments performed by us with a series of lasers indicate that it may be possible to produce stimulated emission from an active medium in melted state.

CONCLUSION

A method of high-temperature stimulated emission spectroscopy was developed and applied to the study of a series of crystals and glasses activated with neodymium ions. The results of this research can be briefly stated as follows:

1. The high-temperature operating limits of seventeen lasers are determined. The experiments show that the most high-temperature resistant are lasers employing mixed fluoride crystals. In particular, the crystals of α-gagarinite and yttrofluorite are capable of generation up to 1000°K[7)].

2. The study of the $E_t(T)$ functions of some crystals revealed a new phenomenon: the effect of high-temperature resonance sensitization of stimulated transitions manifested in the decrease of E_t at high temperatures. Owing to this effect, certain mixed fluoride crystals maintain their output energy characteristics constant within a broad range of temperatures (up to ~400°K and higher).

3. At high temperatures we also observed the flare-up of stimulated transitions (LaF_3–Nd^{3+}), similar in nature to the effect of temperature sensitization, that enabled us to record a new generation line; this line in

7) Our most recent research showed that six more crystals activated with Nd^{3+} will lase at high temperatures. The following are their parameters at 300°K: CaF_2–SrF_2 – λ = 10370 Å, $E_t \approx 100$ J; SrF_2 Type I – λ = 10371 Å, E_t = 43 J and λ = 10448 Å, E_t = 200 J; LaF_3–SrF_2 – λ = 10486 Å, E_t = 11 J and λ = 10635 Å, E_t = 5.5 J; CeF_3 – λ = 10410 Å, E_t = 7 J and λ = 10638 Å, E_t = 8 J; YVO_4 – λ = 10664 Å, E_t = 4 J and λ = 10641 Å, E_t = 100 J; 5NaF-9YF_3 – λ = 10506 Å, E_t = 33 J and λ = 10595 Å, E_t = 60 J. The results of investigation of these materials will be published elsewhere.

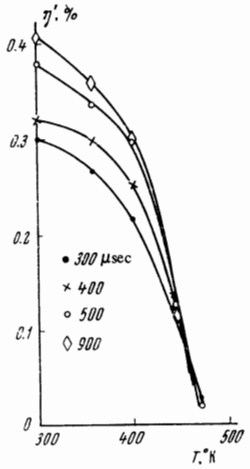

FIG. 15. Thermal dependences of efficiency for the LGS-6 neodymium glass laser (~6% Nd_2O_3).

principle cannot be excited at room and lower temperatures.

The analysis of the observed phenomena allowed us to assume that these effects are connected with phonon resonance oscillations occurring in crystals at high temperatures (near T_D). The nature of these effects are no longer effective. It appears that the analysis of the "generating" centers is in this case possible only in the generation mode.

4. The high-temperature spectra of stimulated emission of seventeen lasers employing crystals and glasses were studied. These studies showed that the widths of the generation lines in the majority of the crystals undergo a negligible change with increased temperature. The analysis of generation spectra also showed that thermal frequency tuning of laser emission is possible within a definite temperature interval. Lasers featuring the KGSS-7 ($\Delta\lambda/\Delta T \approx 0.15$ Å/deg) and LGS-6 ($\Delta\lambda/\Delta T \approx 0.33$ Å/deg) glasses are outstanding in this respect. The high-temperature spectroscopic research also enabled us to discover the effect of stimulated emission line narrowing in glasses and certain mixed fluoride crystals that constitutes an additional confirmation of the autoresonant mechanism of energy migration among various optical centers[2].

5. The high-temperature experiments revealed new stimulated transitions: the G line at $\lambda = 10628$ Å (CaF_2 Type I), the C line at $\lambda = 10623$ Å (CaF_2–SrF_2–BaF_2–YF_3–LaF_3), and the C line at $\lambda = 10591$ Å (LaF_3).

6. The analysis of experimental plots of the $E_t(T)$ functions established that the processes occurring in excited state are similar in nature (parallelism of the $E_t(T)$ plots) within a defined temperature interval (400–800°K) in the majority of the investigated crystals.

7. Investigation of the thermal dependence of efficiency in mixed fluoride and glass lasers showed that η' depends significantly on the length of the pumping light pulse; this further validates the process of energy migration among the optical centers. In the mixed fluoride crystals the probability of energy transfer increases at temperatures close to T_D.

8. In spite of its simplificyt the above method of high-temperature spectroscopy of stimulated emission yields interesting information on the processes taking place in crystals during generation. It seems to us that this methodology is particularly valuable for the study of mixed crystals characterized by broad bands in the optical spectra where the usual spectroscopic methods

In conclusion the author thanks Kh. S. Bagdasarov, S. Kh. Batygov, M. V. Dmitruk, V. V. D'yachenko, G. Ya. Kolodnoĭ, R. G. Mikaelyan, V. V. Osiko, and B. P. Sobolev for the crystals and glasses furnished for the experiments, and V. P. Makarov, V. Ya. Khaimov-Mal'kov, and V. N. Shpakov for discussion of results.

[1] A. A. Kaminskiĭ and V. V. Osiko, Izv. AN SSSR, seriya neorg. mater. 1, 2049 (1965).
[2] A. A. Kaminskiĭ and V. V. Osiko, Ibid. 3, 417 (1967).
[3] E. Snitzer, Appl. Optics 5, 1487 (1966).
[4] G. O. Karapetyan and A. L. Reĭshakhrit, Izv. AN SSSR, seriya neorg. mater. 3, 217 (1967).
[5] T. Kushida, J. Phys. Soc. Japan 22, 351 (1967).
[6] S. Kh. Batygov and A. A. Kaminskiĭ, Zh. Eksp. Teor. Fiz. 53, 839 (1967) [Sov. Phys.-JETP 26, 512 (1961)].
[7] A. A. Kaminskiĭ, ZhETF Pis. Red. 6, 615 (1967) [JETP Lett 6, 115 (1967)].
[8] Yu. K. Voronko, V. V. Osiko, V. T. Udovenchik, and M. M. Fursikov, Fiz. Tverd. Tela 7, 267 (1965) [Sov. Phys.-Solid State 7, 204 (1965)].
[9] D. Stockbarger, J. Opt. Soc. Amer. 39, 1620 (1949).
[10] L. S. Garashina, E. G. Ippolitov, B. M. Zhigarnovskiĭ, and B. P. Sobolev, Issledovanie prirodnogo i tekhnicheskogo mineraloobrazovaniya (A Study of Natural and Synthetic Mineral Formation), Nauka, 1966, p. 289.
[11] A. A. Kaminskiĭ, L. S. Kornienko, and A. M. Prokhorov, Zh. Eksp. Teor. Fiz. 48, 476 (1965) [Sov. Phys. JETP 21, 318 (1965)].
[12] Yu. K. Voronko, A. A. Kaminskiĭ, L. S. Kornienko, V. V. Osiko, A. M. Prokhorov, and V. T. Udovenchik, ZhETF Pis. Red. 1, No. 2, 3 (1965) [JETP Lett. 1, 39 (1965)].
[13] A. A. Kaminskiĭ, V. V. Osiko, A. M. Prokhorov, and Yu. K. Voronko, Phys. Rev. Lett. 22, 419 (1966).
[14] Yu. K. Voron'ko, A. A. Kaminskiĭ, V. V. Osiko, and M. M. Fursikov, Kristallografiya 11, 936 (1966) [Sov. Phys.-Cryst. 11, 793 (1967)].
[15] Yu. K. Voronko, A. A. Kaminskiĭ, and V. V. Osiko, ibid. 13, No. 2 (1968) [13, No. 2 (1968)].
[16] A. A. Kaminskiĭ, V. V. Osiko, and V. T. Udovenchik, Zh. prikl. spektroskop. 6, 40 (1967).
[17] Kh. S. Bagdasarov, Yu. K. Voron'ko, A. A. Kaminskiĭ, and V. V. Osiko, Izv. AN SSSR, seriya neorg. mater. 1, 2088 (1965).
[18] Kh. S. Bagdasarov, A. A. Kaminskiĭ, Ya. E. Lansker, and B. P. Sobolev, ZhETF Pis. Red. 5, 220 (1967) [JETP Lett. 5, 175 (1967)].
[19] A. A. Kaminskiĭ, Ya. E. Lapsker, and B. P. Sobolev, Phys. Stat. Sol. 23, K5 (1967).
[20] L. F. Johnson, J. Appl. Phys. 34, 897 (1963).
[21] G. M. Zverev and G. Ya. Kolodnyĭ, Zh. Eksp. Teor. Fiz. 52, 337 (1967) [Sov. Phys.-JETP 25, 217 (1967)].
A. A. Morozov, P. P. Feofilov, M. N. Tolstoĭ, and V. N. Shapovalov, Opt. Spektrosk. 22, 414 (1967).

[22] A. A. Kaminskiĭ, Zh. Eksp. Teor. Fiz. 51, 49 (1966) [Sov. Phys.-JETP 24, 33 (1967)].
[23] V. P. Preobrazhenskiĭ, Teplotekhnicheskie izmereniya i pribory (Heat Engineering Measurements and Instruments), Gosenergoizdat, 1946.
[24] A. A. Kaminskiĭ, V. V. Osiko, and M. M. Fursikov, ZhETF Pis. Red. 4, 92 (1966) [JETP Lett. 4, 62 (1966)].
[25] A. A. Kaminskii, Phys. Stat. Sol. 20, K51 (1967).
[26] A. A. Kaminskiĭ, L. S. Kornienko, and A. M. Prokhorov, Zh. Eksp. Teor. Fiz. 48, 1262 (1965) [Sov. Phys. JETP 21, 844 (1965)].
[27] Yu. K. Voron'ko, A. A. Kaminskiĭ, V. V. Osiko, and A. M. Prokhorov, Izv. AN SSSR, seriya neorg, mater. 2, 1161 (1966).
[28] Yu. K. Voron'ko, A. A. Kaminskiĭ, and V. V. Osiko, Zh. Eksp. Teor. Fiz. 49, 420 (1965) [Sov. Phys.-JETP 22, 295 (1966)].
[29] M. V. Dmitruk and A. A. Kaminskiĭ, Zh. Eksp. Teor. Fiz. 53, 874 (1967). [Sov. Phys.-JETP 26, 531 (1968)].
[30] Kh. S. Bagdasarov, Yu. K. Voron'ko, A. A. Kaminskiĭ, L. V. Krotova, and V. V. Osiko, Phys. Stat. Sol. 12, 905 (1965).
[31] A. A. Kaminskiĭ, Yu. K. Voron'ko, and V. V. Osiko, Phys. Stat. Sol. 21, K21 (1967).
[32] M. A. El'yashevich, Atomnaya i molekulyarnaya spektroskopiya (Atomic and Molecular Spectroscopy), Fizmatgiz, 1962.
[33] Metody rascheta opticheskikh kvantovykh generatorov (Methods of Laser Analysis) 1, Nauka i technika, Minsk, 1966.
[34] A. Yariv and J. P. Gordon, Proc. IEEE 51, 3 (1963).
[35] A. A. Mak, Yu. A. Anan'ev, and B. A. Ermakov, Usp. Fiz. Nauk 92, 373 (1967) [Sov. Phys.-Usp. 419 (1968)].
[36] F. I. Fedorov, Teoriya uprugikh voln v kristallakh (Theory of Elastic Waves in Crystals), Nauka, 1965. T. G. Bystrova and F. I. Fedorov, Kristallografiya 12, 11 and 560 (1967) [Sov. Phys.-Crystall. 12, 9 (1967) and 12, 493 (1968)].
[37] H. B. Huntington, Solid State Physics 7, 213 (1958).
[38] J. M. Ziman, Electrons and Phonons, 1960.
[39] P. Debye, Ann. Physik 39, 789 (1910).
[40] D. R. Huffman and N. H. Norwood, Phys. Rev. 117, 709 (1960).
[41] D. Gerlich, Phys. Rev. 136, A1366 (1964).
[42] D. Gerlich, Phys. Rev. 135, A1331 (1964).
[43] W. M. Yen, W. C. Scott, and A. L. Schawlow, Phys. Rev. 136, A271 (1964).
[44] A. Kiel, Electron. Quant. 3 Conf. Internat. Paris, 1964, p. 765.
[45] L. F. Johnson and R. A. Thomas, Phys. Rev. 131, 2038 (1963).
[46] D. W. Goodwin, Z. Angew. Math. Physik 16, 35 (1965. E. G. Spenser, R. T. Denton, T. B. Bateman, W. R. Snow, and L. G. Van Uiter, J. Appl. Phys. 34, 3059 (1963).
[47] A. A. Kaminskiĭ and V. N. Shpakov, Zh. Eksp. Teor. Fiz. 52, 103 (1967) [Sov. Phys.-JETP 25, 67 (1967)].

Translated by S. Kassel
87